

Received September 27, 2016, accepted November 4, 2016, date of publication November 11, 2016, date of current version November 28, 2016.

Digital Object Identifier 10.1109/ACCESS.2016.2628044

Design of a Wideband Circularly Polarized Strip-Helical Antenna With a Parasitic Patch

XIHUI TANG¹, YEJUN HE¹, AND BOTAO FENG²

¹Shenzhen Key Laboratory of Antennas and Propagation, College of Information Engineering, Shenzhen University, Shenzhen 518060, China

²Shenzhen Key Laboratory of Antennas and Propagation, College of Electronic Science and Technology, Shenzhen University, Shenzhen 518060, China

Corresponding author: X. Tang (tangxh_2009@126.com)

This work was supported in part by the Natural Science Foundation of China under Grant 61301075 and in part by the Shenzhen Key Laboratory of Antennas and Propagation under Grant ZDSYS201507031550105. The work of B. Feng was supported in part by the Natural Science Foundation of Guangdong Province, China, under Grant 2016A030310056, in part by the Key Project of Department of Education of Guangdong Province under Grant 2015KTSCX123, in part by the Fundamental Research Foundation of Shenzhen under Grant JCYJ2016 3146, and in part by the Natural Science Foundation of SZU under Grant 2016021.

ABSTRACT A wideband strip-helical antenna with a parasitic circular patch for circular polarization is designed in this paper. A strip-helix with 2.5 turns and a pitch angle of 5° is placed over a ground plane and coaxial probe-fed by a $50\text{-}\Omega$ SMA connector. A parasitic patch is electromagnetic-coupled to the open end of the strip-helix with an extremely small distance. By combining the strip-helix with the parasitic patch, two nearby circularly polarized (CP) resonances are produced and a wide axial ratio (AR) bandwidth is obtained. The strip-helix can excite a CP resonance in axial mode, while the parasitic patch can generate another nearby one in fundamental mode. Radiation characteristics of the proposed design, including current distributions, reflection coefficient (S_{11}), AR, and radiation patterns, are studied. Measured results shows that the proposed antenna has an impedance bandwidth ($S_{11} \leq -10$ dB) of 53%, an AR bandwidth ($AR \leq 3$ dB) of 44%, and a peak gain of 9.4 dBi in its volume of $0.43\lambda_0 \times 0.43\lambda_0 \times 0.25\lambda_0$, where λ_0 is the wavelength in free space at the center operation frequency.

INDEX TERMS Strip-helical antenna, patch, wideband, circular polarization.

I. INTRODUCTION

In recent years, wideband CP antennas have received a lot of research, since they can satisfy the requirement of the high speed transmission for wireless communication terminals. Conventional axial-mode wire helical antennas, [1], known as a type of travelling wave antennas, have excellent CP performances. Unfortunately, these helical antennas are not suitable for compact terminals due to their large axial height. To solve this problem, some helical antennas with few numbers of turns and small pitch angles [2], [3] have been reported by H. Nakano, e.g., a low-profile helix with two turns and pitch angle of 4° in [2] has an AR bandwidth ($AR \leq 3$ dB) of 12%. Moreover, a hemispherical helical antenna [4], designed by H. T. Hui, has improved the AR bandwidth up to 15%. A tapered strip-helical antenna in [5] has further increased the AR bandwidth to 24% with an antenna height of $0.28\lambda_0$, where λ_0 is the free space wavelength at the center operation frequency. Generally, one condition should be fulfilled that the reflected currents from the open end of the helix are fewness and negligible at operation frequencies for these

low-profile helical antennas with CP radiation. On the other hand, single-fed CP microstrip patch antennas [6] are one type of resonant antennas and have many advantageous features, such as low-profile, easy to fabrication and symmetric radiation patterns. But their AR bandwidths are narrow. In [7]–[10], some techniques have been introduced for enhancing the AR bandwidth, e.g., a wide AR bandwidth of 34% is obtained by using aperture-fed rotated stacked patches with an antenna height of $0.35\lambda_0$ [9]. Some helical/spiral excited CP dielectric resonator antennas (DRAs) with compact size have been proposed in [11]–[13]. For example, the helical excited DRA in [11] has an AR bandwidth of $\sim 13\%$, and the spiral slot excited DRA in [13] has an AR bandwidth of $\sim 25\%$. In addition, there are two other types of wideband CP antennas with a similar antenna height of $0.25\lambda_0$ reported in [14] and [15]. Their AR bandwidths are 34% and 27%, respectively. Note that a planar CP helical antenna has been designed in [16] with an AR bandwidth of 34% and a low-profile of $0.11\lambda_0$. However, its area is $1.23\lambda_0 \times 0.77\lambda_0$ and the gain varies greatly from 3.1 dBi to 10.5 dBi over the

AR bandwidth. Not long ago, some wideband strip-helical antennas with AR bandwidths of $\sim 50\%$ have been presented in [17] and [18]. Even so, their antenna heights of $\sim 0.5\lambda_0$ are not low-profile.

Technologically, adding parasitic element [19], [20] is an effective method of improving AR bandwidth for helical antennas. A strip-helical antenna with a parasitic patch has been reported in [20]. Nevertheless, the AR bandwidth of the strip-helical antenna is only 15%, since the EM-coupling level between the strip-helix and the parasitic patch is not high. In our previous work [21], a new type of wideband strip-helical antenna with a parasitic circular patch has been analyzed numerically. The EM-coupling is strong enough such that both the strip-helix and the parasitic patch can generate a CP resonance and an outstanding AR bandwidth of 44% is obtained. In this paper, both simulation and measurement are carried out to verify the features of the proposed strip-helical antenna, such as wide CP bandwidth, high gain and stable radiation patterns. A detailed study is also added to explain the radiation mechanism of the proposed antenna. Moreover, a comparison between the proposed antenna and those related antennas in [9], [10], [14]–[18], and [20] is implemented to demonstrate the advantages of the proposed antenna.

II. DESIGN PROCEDURE

Fig. 1 shows the geometry of the proposed strip-helical antenna. The antenna structure consists of a strip-helix, a circular patch, a square ground plane and a $50\ \Omega$ SMA connector. The strip-helix is rolled in right hand direction for right-hand circular polarization (RHCP). It is made of horizontal strip with uniform width (w) of $12\ \text{mm}$. With the aim of obtaining a low-profile structure, the pitch angle (α) has a small value of 5° and the numbers of the turns (n) is selected to be 2.5. The radius of the helix (the distance from Z-axis to the center of the strip) (R) is equal to $30\ \text{mm}$, such that the circumference of one turn of the strip-helix ($C = 2\pi R$) is about 1λ of $1.5\ \text{GHz}$. The corresponding spacing between turns (S) is equal to $15\ \text{mm}$ ($S = C \tan \alpha$). The circular patch with a radius (r) of $24\ \text{mm}$ is placed over the strip-helix as a parasitic device, which has an extremely small distance (h_2) of $0.5\ \text{mm}$ to the open end of the strip-helix. The center of the parasitic patch is set to be along the y-axis and has a distance of D_y to the axis of the strip-helix. This placement can result in strongly coupling between the parasitic patch and the strip-helix, since the radius of the parasitic patch (r) is smaller than the radius of the strip-helix (R). The square ground plane is printed on the bottom layer of the F4BM2 substrate with a relative permittivity of $\epsilon_{r1} = 2.2$, and a thickness of $h_1 = 3\ \text{mm}$. It has a length of $G = 130\ \text{mm}$ and is used to suppress back radiation. The SMA connector is laid under the ground plane. The inner of the SMA connector with a diameter of $1\ \text{mm}$ is connected with the strip helix. The height (H) of the whole antenna structure is equal to $41\ \text{mm}$.

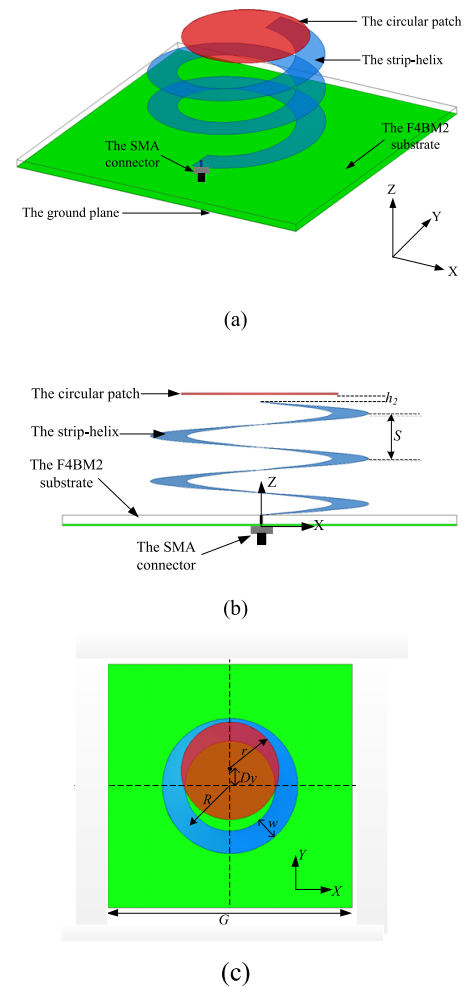


FIGURE 1. Geometry of the proposed strip-helical antenna with a parasitic patch. (a) 3D view, (b) Side view, (c) Top view.

A. THE STRIP-HELIX WITHOUT THE PARASITIC PATCH

In design procedure, we firstly employ a strip-helix as the radiator of the proposed antenna. There are four independent parameters of the strip-helix, α , R , w and n . The parameter α is to be as small as possible for reducing the antenna height. The parameter R controls the operation frequency of the strip-helix. The other two parameters, w and n , play major roles in antenna performances and deserve to be studied numerically. The numerical results are obtained with the aid of the simulation software 'HFSS'.

Fig. 2 demonstrates the reflection coefficient (S_{11}) and the AR against frequency of the strip-helix with different values of w . The reflection coefficient is significantly improved when w is increased from $4\ \text{mm}$ to $20\ \text{mm}$. An impedance bandwidth ($S_{11} \leq -10\ \text{dB}$) from $1.25\ \text{GHz}$ to $1.65\ \text{GHz}$ is obtained as long as w is not less than $12\ \text{mm}$. On the other hand, the minimum value of the AR is less than $1\ \text{dB}$ at $1.45\ \text{GHz}$ when w is $12\ \text{mm}$. Considering the performances on both reflection coefficient and AR, the parameter w is optimized to be $12\ \text{mm}$.

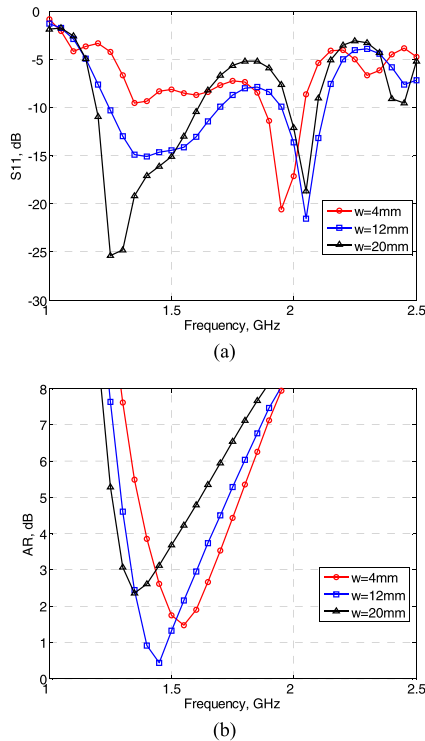


FIGURE 2. Reflection coefficient (S_{11}) and axial ratio against frequency of the strip-helix with different values of w . (a) Reflection coefficient, (b) Axial ratio.

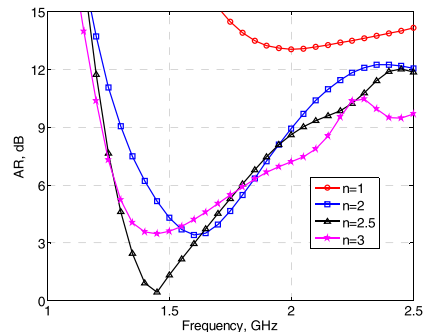


FIGURE 3. Axial ratio against frequency of the strip-helix with different values of n .

Fig. 3 exhibits the AR against frequency when n is 1, 2, 2.5 and 3, respectively. It is noticed that the strip-helix can not excite a CP wave when n is 1. Thus, we increase the parameter n to 2, or 3. In spite of this, the strip-helix can not excite a pure CP wave yet, since the AR is larger than 3 dB. It is probably caused by the reflected currents at the open end of the strip-helix, which deteriorate the decaying form of the travelling currents along strip-helix. Hence, it is necessary to adjust n to reduce the reflected currents for achieving a good CP radiation. The minimum value of the AR drops to 0.43 dB at 1.475 GHz when n is optimized to be 2.5. And a 3-dB AR bandwidth of 17% (1.35 GHz - 1.6 GHz) is observed.

In order to analyzing the operation principle of the strip-helix, the magnitude of the current densities (J_{surf}) on the

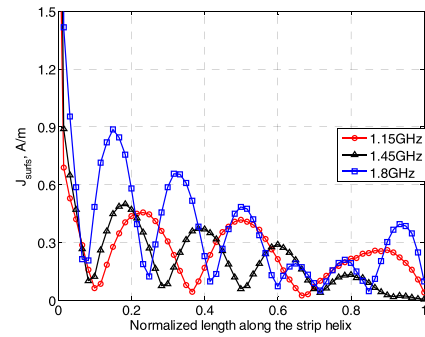


FIGURE 4. Current densities on the center of the strip along the helix without the parasitic patch at different frequencies.

center of the strip along the helix at different frequencies of 1.15 GHz, 1.45 GHz, and 1.8 GHz is illustrated in Fig. 4. The forward travelling currents decay from the feed end to the open end of the strip-helix at all three frequencies. Furthermore, the backward reflected currents at the open end of strip-helix are negligible at 1.45 GHz. While they exist obviously and interfere the forward travelling currents at both 1.15 GHz and 1.8 GHz. This phenomenon indicates that one condition must be satisfied that the reflected currents at the open end are few and negligible for the strip-helix with good CP radiation. Unfortunately, this condition is fulfilled in a narrow frequency range.

B. IMPROVEMENT OF AR BANDWIDTH

As is shown in Section A, the reflected currents at the open end of the strip-helix damage the purity of CP radiation and limits the AR bandwidth. Then, it is desirable to introduce an effective technique for increasing the AR bandwidth significantly without deteriorating the remaining characteristics of the strip-helix. Considering the fact that the strip-helix works in a resonance mode with circular polarization, we plan to bring in an additional device for exciting another nearby CP resonance. As is well known, a microstrip patch can easily acquire a wide bandwidth in its fundamental mode by utilizing an EM-coupled feeding technique, such as the L-shaped probe fed technique. In case the feeding technique can provide the conditions of CP radiation, the microstrip patch will correspondingly excite a CP wave, e.g., the dual/multi fed CP microstrip patch antenna. Accordingly, a parasitic circular patch is EM-coupled to the strip-helix. In Fig. 3, the value of axial ratio with n equal to 2.5 is about 9 dB at 2 GHz. It means that the strip-helix provides an approximate CP signal. Once the parasitic patch with right size resonances in fundamental mode at this frequency, a good CP wave might be generated by the interaction of the strip-helix and the parasitic patch.

The effectiveness of the parasitic patch on improving the AR bandwidth is evaluated. The parameter r is estimated to be in the range of 20 mm to 30 mm with the aim of exciting the fundamental mode of the parasitic patch at around 2 GHz. While the parameter h_2 should be as small as possible for

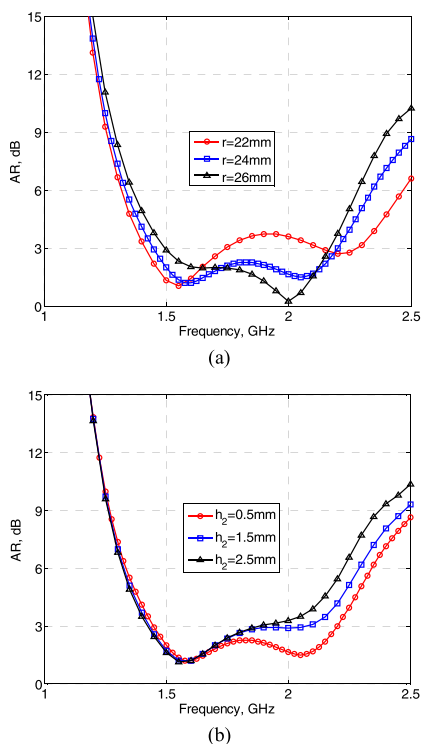


FIGURE 5. Axial ratio against frequency of the proposed antenna with different values of r and h_2 . (a) various r , $h_2 = 0.5$ mm, (b) various h_2 , $r = 24$ mm.

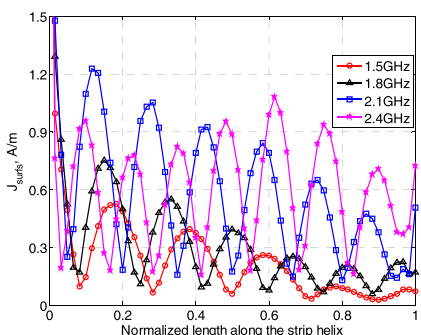


FIGURE 6. Current densities on the center of the strip along the helix with the parasitic patch at different frequencies.

achieving strongly coupling. Fig. 5 shows the AR against frequency with different values of r and h_2 . It is clearly seen that two CP resonances are generated by the strip-helix together with the parasitic patch. The lower CP resonance is at ~ 1.5 GHz while the upper CP resonance is at ~ 2 GHz. In Fig. 5(a), the upper resonance shifts from 2.25 GHz to 2 GHz when r is increased from 22 mm to 26 mm. r is determined to be 24 mm in order to obtaining a wide 3-dB AR bandwidth of 41% (1.45 GHz to 2.2 GHz). In Fig. 5(b), the value of the AR at 2 GHz drops from 3.3 dB to 1.6 dB when h_2 is decreased from 2.5 mm to 0.5 mm, since the EM-coupling is significantly enhanced with the decrease of h_2 . Therefore, h_2 is fixed to 0.5 mm.

Fig. 6 depicts the magnitude of the current densities (J_{surf}) on the center of the strip along the helix with the

parasitic patch at different frequencies of 1.5 GHz, 1.8 GHz, 2.1 GHz and 2.4 GHz. The forward travelling currents decay from the feed end to the open end of the strip-helix with negligible backward reflected currents at 1.5 GHz. It is similar with that one without the parasitic patch. The reflected currents are increased when the operation frequency shifts from 1.5 GHz to 2.4 GHz. The state of the currents changes from a travelling mode to a standing-travelling mode correspondingly. It is due to the raise of the EM-coupling between the strip-helix and the parasitic patch. In order to investigating the effect of the parasitic patch on radiation characteristic at lower frequency, Fig. 7 compares the simulated radiation patterns of the proposed strip-helical antenna with and without the parasitic patch at 1.45 GHz. The Co-Polarization is very similar to each other. While the X-Polarization is increased by the interaction of the strip-helix and the parasitic patch. On the other hand, the current distributions on the parasitic patch at 2.1 GHz are shown in Fig. 8. It is observed that a CP wave is excited from the parasitic patch at 2.1 GHz. The current flows in a counterclockwise direction, which will contribute to an RHCP.

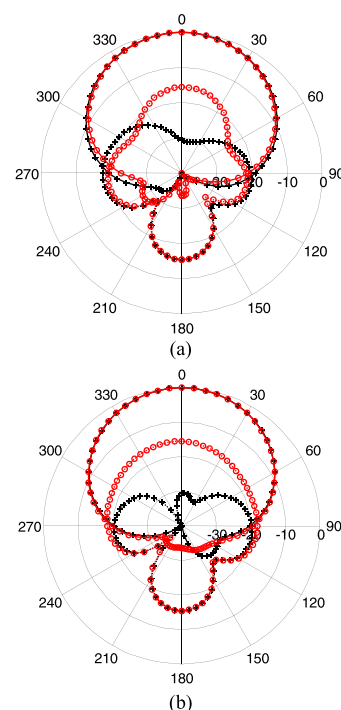


FIGURE 7. Simulated radiation patterns of the proposed strip-helical antenna with and without the parasitic patch at 1.45 GHz. Black line: without the parasitic patch, red line: with the parasitic patch. Solid line: RHCP, dash line: LHCP. (a) $\phi = 0^\circ$ plane, (b) $\phi = 90^\circ$ plane.

In summary, the lower CP resonance is excited from the strip-helix while the upper CP resonance is excited from the parasitic patch. More importantly, they are almost independent of each other. This feature is convenient for designing the proposed antenna. Based on the analysis of the operation principle, some design guidelines are summarized as follows.

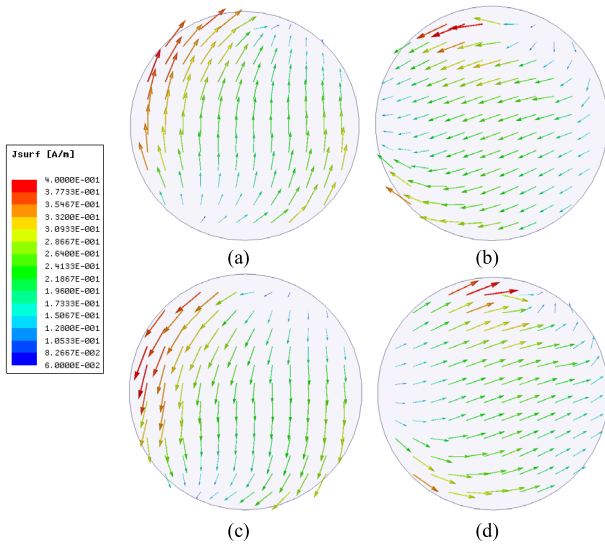


FIGURE 8. Current distributions on the parasitic patch of the proposed antenna at 2.1 GHz at four phase angles. (a) 0°, (b) 90°, (c) 180°, (d) 270°.

- 1) The increase in the width (w) of the strip-helix benefits the reflection coefficient of the proposed antenna.
- 2) The circumference ($2\pi R$) of the strip-helix is calculated as $2\pi R \approx \lambda_l$, where λ_l is the wavelength in free space at the lower CP resonance.
- 3) The value of the AR at the lower CP resonance can be optimized by adjusting the numbers (n) of the turns of the strip-helix.
- 4) The diameter ($2r$) of the parasitic patch correspond to the frequency of the upper CP resonance.
- 5) The decrease in the distance (h_2) between the parasitic patch and the open end of the strip-helix is directly proportional to the decrease in AR at the upper CP resonance.

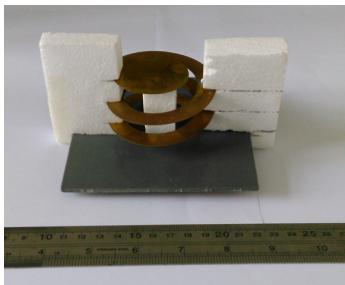


FIGURE 9. View of the prototype of the proposed antenna.

III. RESULTS AND COMPARISONS

A prototype of the proposed antenna is fabricated and shown in Fig. 9. Both the strip-helix and the parasitic patch are supported by foam with a relatively permittivity of 1. The antenna performances are measured by the E5071C Network Analyzer and the Near Field Antenna Measurement System, Satimo. Measurement results of reflection coefficient, AR,

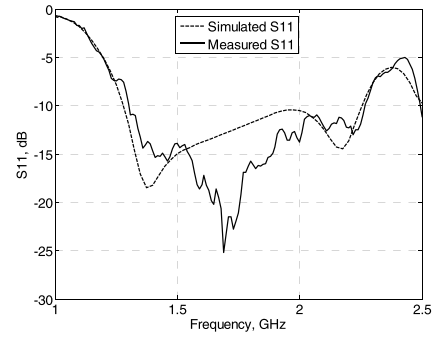


FIGURE 10. Reflection coefficient (S_{11}) against frequency of the proposed antenna.

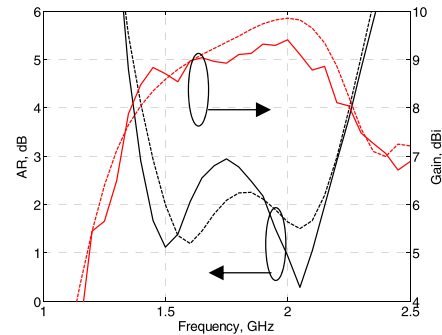


FIGURE 11. Axial ratio and gain against frequency of the proposed antenna. Solid line: measured data, dash line: simulated data.

gain and radiation patterns are presented and compared with the corresponding simulated results.

Fig. 10 demonstrates the reflection coefficient against frequency. The proposed antenna has simulated and measured impedance bandwidths ($S_{11} \leq -10$ dB) of 56% (1.275 GHz to 2.25 GHz) and 53% (1.31 GHz to 2.26 GHz), respectively. The minimum value of reflection coefficient in measurement is 25 dB at 1.69 GHz. The AR and gain against frequency are described in Fig. 11. A good agreement between the simulated and measured results is observed. From the W-shaped AR curves, it is clearly seen that two nearby CP resonances are generated. Therefore, wide AR bandwidths ($AR \leq 3$ dB) of 41% (1.45 GHz to 2.2 GHz) and 44% (1.4 GHz to 2.2 GHz) are obtained in simulation and measurement, which are overlapped by their corresponding impedance bandwidths. The normalized circumferences of C/λ varies from 0.88 to 1 over the measured AR bandwidth, where C is the circumference of one turn of the strip-helix. The volume of the proposed antenna is $0.43\lambda_0 \times 0.43\lambda_0 \times 0.25\lambda_0$, where λ_0 is the wavelength in free space at the center operation frequency of 1.8 GHz. The measured gain is slightly less than the simulated one. This variance might be caused by the additional loss introduced by the SMA connector and the alignment error of the measurement setup. The measured gain is stable with 9 ± 1 dBi and has a peak value of 9.4 dBi at 2 GHz over the AR bandwidth.

Fig. 12 depicts the simulated and measured radiation patterns at 1.45 GHz, 1.8 GHz and 2.2 GHz, respectively.

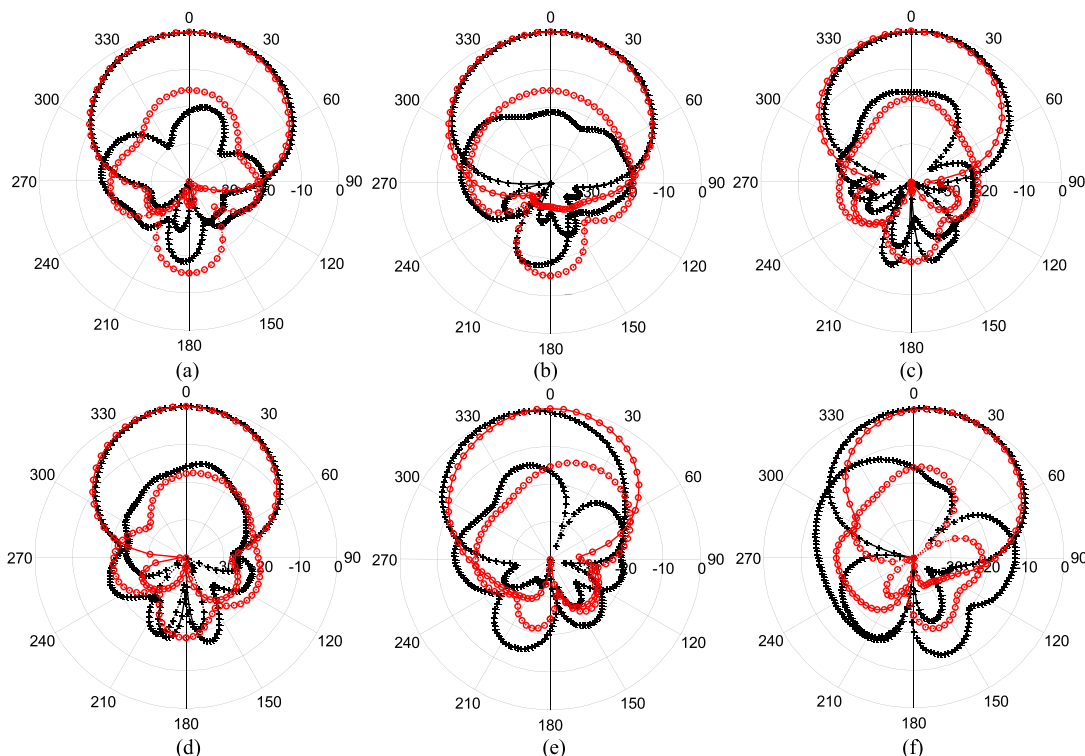


FIGURE 12. Simulated and measured radiation patterns of the proposed antenna at 1.45 GHz, 1.8 GHz and 2.2 GHz, respectively. Black line: measured data, red line : simulated data. Solid line: RHCP, dash line : LHCP. (a) $f = 1.45$ GHz, $\varphi = 0^\circ$ plane, (b) $f = 1.45$ GHz, $\varphi = 90^\circ$ plane, (c) $f = 1.8$ GHz, $\varphi = 0^\circ$ plane, (d) $f = 1.8$ GHz, $\varphi = 90^\circ$ plane, (e) $f = 2.2$ GHz, $\varphi = 0^\circ$ plane, (f) $f = 2.2$ GHz, $\varphi = 90^\circ$ plane.

TABLE 1. Performance comparisons of wideband cp antennas.

Ref.	Area	Height	AR bandwidth (AR ≤ 3 dB)	Peak gain, dB	Gain over the AR bandwidth, dB
[9]	$0.62\lambda_0 \times 0.62\lambda_0$	$0.35\lambda_0$	34%	~ 9	6–9
[10]	$0.64\lambda_0 \times 0.64\lambda_0$	$0.13\lambda_0$	24%	~ 9	8 ± 1
[14]	$0.47\lambda_0 \times 0.47\lambda_0$	$0.27\lambda_0$	34%	7.6	5.2–7.6
[15]	$0.45\lambda_0 \times 0.45\lambda_0$	$0.24\lambda_0$	27%	6.8	6 ± 1
[16]	$1.23\lambda_0 \times 0.77\lambda_0$	$0.11\lambda_0$	34%	10.5	3.1–10.5
[17]	$0.45\lambda_0 \times 0.45\lambda_0$	$0.45\lambda_0$	58%	~ 10	9 ± 1
[18]	$0.40\lambda_0 \times 0.40\lambda_0$	$0.52\lambda_0$	46%	~ 8	7.5 ± 0.5
[20]	$0.35\lambda_0 \times 0.35\lambda_0$	$0.35\lambda_0$	15%	~ 10	9.5 ± 0.5
Proposed	$0.43\lambda_0 \times 0.43\lambda_0$	$0.25\lambda_0$	44%	9.4	9 ± 1

Simulated and measured results are in good agreement as well. The proposed antenna is of right-hand circular polarization. The radiation patterns are very symmetric with respect to the axial direction at 1.45 GHz and 1.8 GHz, since the symmetric strip-helix is the main radiator at lower frequencies. As the operation frequency increases to 2.2 GHz, the direction of maximum radiation slightly deviates from the axial direction with tilt angle of $\pm 10^\circ$ at the two principle planes: $\varphi = 0^\circ$ and $\varphi = 90^\circ$. It is probably due to the biasing location of the parasitic patch along y-axis. Furthermore, the front-to-back ratio is more than 15 dB and the half power beamwidths (HPBW)s are about 70° over the AR bandwidth.

Table 1 shows the performance comparisons between the proposed antenna and other types of wideband CP antennas

in [9], [10], [14]–[18], and [20]. Although the planar helical antenna in [16] has a wide AR bandwidth of 34% with an antenna height of $0.11\lambda_0$, its planar area is 5 times of that of the proposed one and the stability of gain over the AR bandwidth is poor. More importantly, the AR bandwidth of the proposed antenna is 3 times of that with similar antenna structure in [20].

IV. CONCLUSION

A new technique is proposed for improving AR bandwidth of a strip-helical antenna with circular polarization. By employing a parasitic circular patch over a strip-helix, two nearby CP resonances are produced and an outstanding AR bandwidth

of 44% is obtained. The working principle of the proposed antenna has been analyzed based on the current distributions on the strip-helix and the parasitic patch. The strip-helix not only generates a CP radiation alone at the lower resonance, but also acts as a feeding device at the upper resonance, where the parasitic patch excites a CP wave in fundamental mode. In addition, some crucial design guidelines are summarized for antenna engineers. Owing to these advantages of easy to design, wide operation bandwidth, stable radiation patterns and high gain, the proposed antenna is a good candidate for broadband CP radiation.

REFERENCES

- [1] J. D. Kraus, "The helical antenna," *Proc. IRE*, vol. 37, no. 3, pp. 263–272, 1949.
- [2] H. Nakano, H. Takeda, T. Honma, H. Mimaki, and J. Yamauchi, "Extremely low-profile helix radiating a circularly polarized wave," *IEEE Trans. Antennas Propag.*, vol. 39, no. 6, pp. 754–757, Jun. 1991.
- [3] H. Nakano, S. Okuzawa, K. Ohishi, H. Mimaki, and J. Yamauchi, "A curl antenna," *IEEE Trans. Antennas Propag.*, vol. 41, no. 11, pp. 1570–1575, Nov. 1993.
- [4] H. T. Hui, K. Y. Chan, and E. K. N. Yung, "The low-profile hemispherical helical antenna with circular polarization radiation over a wide angular range," *IEEE Trans. Antennas Propag.*, vol. 51, no. 6, pp. 1415–1418, Jun. 2003.
- [5] H. W. Alsawaha and A. Safaai-Jazi, "Ultrawideband hemispherical helical antennas," *IEEE Trans. Antennas Propag.*, vol. 58, no. 10, pp. 3175–3181, Oct. 2010.
- [6] I. J. Bahl and P. Bhartia, *Microstrip Antennas*. New York, NY, USA: Artech House, 1980.
- [7] K. L. Chung, "A wideband circularly polarized H-shaped patch antenna," *IEEE Trans. Antennas Propag.*, vol. 58, no. 10, pp. 3379–3383, Oct. 2010.
- [8] Z. Wang, S. Fang, S. Fu, and S. Jia, "Single-fed broadband circularly polarized stacked patch antenna with horizontally meandered strip for universal UHF RFID applications," *IEEE Trans. Microw. Theory Techn.*, vol. 59, no. 4, pp. 1066–1073, Apr. 2011.
- [9] H. Oraizi and R. Pazoki, "Wideband circularly polarized aperture-fed rotated stacked patch antenna," *IEEE Trans. Antennas Propag.*, vol. 61, no. 3, pp. 1048–1054, Mar. 2013.
- [10] J. Wu, Y. Yin, Z. Wang, and R. Lian, "Broadband circularly polarized patch antenna with parasitic strips," *IEEE Antennas Wireless Propag. Lett.*, vol. 14, pp. 559–562, 2015.
- [11] A. Motevasselian, A. Ellgardt, and B. L. G. Jonsson, "A helix excited circularly polarized hollow cylindrical dielectric resonator antenna," *IEEE Antennas Wireless Propag. Lett.*, vol. 12, pp. 535–538, 2013.
- [12] L. Zhang, Y.-C. Jiao, and Z.-B. Weng, "Wideband circularly polarized dielectric resonator antenna with a square spiral microstrip feedline," *Prog. Electromagn. Res. Lett.*, vol. 41, pp. 11–20, 2013.
- [13] M. Zou, J. Pan, and Z. Nie, "A wideband circularly polarized rectangular dielectric resonator antenna excited by an archimedean spiral slot," *IEEE Antennas Wireless Propag. Lett.*, vol. 14, pp. 446–449, 2015.
- [14] S.-P. Pan, J.-Y. Sze, and P.-J. Tu, "Circularly polarized square slot antenna with a largely enhanced axial-ratio bandwidth," *IEEE Antennas Wireless Propag. Lett.*, vol. 11, pp. 969–972, 2012.
- [15] Y. He, W. He, and H. Wong, "A wideband circularly polarized cross-dipole antenna," *IEEE Antennas Wireless Propag. Lett.*, vol. 13, pp. 67–70, 2014.
- [16] Z. Chen and Z. Shen, "Planar helical antenna of circular polarization," *IEEE Trans. Antennas Propag.*, vol. 63, no. 10, pp. 4315–4323, Oct. 2015.
- [17] J. N. Mei, D. W. Ding, and G. Wang, "Design of compact wideband circularly polarized conical helix," in *Proc. Int. Conf. Comput. Inf. Syst. Ind. Appl.*, 2015, pp. 139–141.
- [18] X. Tang, B. Feng, and Y. Long, "The analysis of a wideband strip-helical antenna with 1.1 turns," *Int. J. Antennas Propag.*, vol. 2016, Jan. 2016, Art. no. 5950472.
- [19] Z. H. Wu, W. Q. Che, B. Fu, P. Y. Lau, and E. K. N. Yung, "Axial mode elliptical helical antenna with parasitic wire for CP bandwidth enhancement," *IET Microw., Antennas Propag.*, vol. 1, no. 4, pp. 943–948, Aug. 2007.
- [20] S. Fu, Q. Kong, S.-J. Fang, and Z. Wang, "Optimized design of helical antenna with parasitic patch for L-band satellite communications," *Prog. Electromagn. Res. Lett.*, vol. 44, pp. 9–13, 2014.
- [21] X. Tang and Y. Long, "A wideband strip-helical antenna with a parasitic patch," in *Proc. 9th Eur. Conf. Antennas Propag.*, 2015, pp. 1–4.



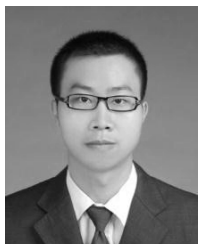
XIHUI TANG was born in Jiangxi province, China, in 1985. He received the B.S. and Ph.D. degree in electronic and communication engineering from Sun Yat-Sen University in 2006 and 2011, respectively. Since 2012, he has been a Faculty Member with Shenzhen University, where he is currently a Lecturer with the Department of Electronic Engineering. His research interests include microstrip antennas, helical antennas, and mobile antennas.



YEJUN HE (SM'09) received the B.S. degree from the Huazhong University of Science and Technology (HUST), Wuhan, China, in 1994, the M.S. degree from the Wuhan University of Technology, Wuhan, in 2002, and the Ph.D. degree from HUST in 2005. From 2005 to 2006, he was a Research Associate with the Department of Electronic and Information Engineering, The Hong Kong Polytechnic University, Hong Kong. From 2006 to 2007, he was a Research Associate with

the Department of Electronic Engineering, Faculty of Engineering, Chinese University of Hong Kong, Hong Kong. In 2012, he was a Visiting Professor with the Department of Electrical and Computer Engineering, University of Waterloo, Waterloo, ON, Canada. From 2013 to 2015, he was an Advanced Visiting Scholar (Visiting Professor) with the School of Electrical and Computer Engineering, Georgia Institute of Technology, Atlanta, GA, USA. Since 2011, he has been a Full Professor with the College of Information Engineering, Shenzhen University, where he is currently the Director of the Shenzhen Key Laboratory of Antennas and Propagation and the Director of the Guangdong Engineering Research Center of Base Station Antennas and Propagation. He has authored or co-authored over 100 research papers, books (chapters) and holds 13 patents. His research interests include channel coding and modulation, 4G/5G wireless mobile communication, space-time processing, antennas, and RF.

Dr. He is serving as an Associate Editor of the IEEE Access and *Security and Communication Networks*. He was the TPC Co-Chair of WCCO 2015. He has served as a Reviewer for various journals such as the IEEE Transactions on Vehicular Technology, the IEEE Transactions on Communications, the IEEE Transactions on Wireless Communications, the IEEE Transactions on Industrial Electronics, the IEEE Wireless Communications, the IEEE Communications Letters, the IEEE Journal on Selected Areas in Communications, the *International Journal of Communication Systems*, the *Wireless Communications and Mobile Computing*, and the *Wireless Personal Communications*. He has also served as a Technical Program Committee Member or a Session Chair for various conferences, including the IEEE Global Telecommunications Conference, the IEEE International Conference on Communications, the IEEE Wireless Communication Networking Conference, and the IEEE Vehicular Technology Conference. He served as an Organizing Committee Vice Chair of International Conference on Communications and Mobile Computing (CMC 2010) and an Editor of CMC2010 Proceedings. He acted as the Publicity Chair of several international conferences such as the IEEE PIMRC 2012. He is the Principal Investigator for over 20 current or finished research projects including NSFC of China, the Guangdong Provincial Science and Technology Programs and the Shenzhen Science and Technology Programs. He is a Senior Member of China Institute of Communications (SM'07) and a Senior Member of China Institute of Electronics (SM'11).



China United Network Communications Co. Ltd., from 2009 to 2012, where

BOTAO FENG (M'14) received the B.S. and M.S. degrees in communication engineering from the Chongqing University of Posts and Telecommunications, Chongqing, China, in 2004 and 2009, respectively, and the Ph.D. degree in communication and information system from the Beijing University of Posts and Telecommunications, Beijing, China, in 2015. He joined the Dongguan Branch of Nokia Mobile Phones Ltd., China, as a Communication Engineer in 2004. He joined

he was involved in the optimization of mobile network. He is currently an Associate Professor, a Postgraduate Advisor, and a Post-Doctoral Advisor with Shenzhen University, Guangdong, China. He is also the head of the Key Laboratory of Wireless Communication, Antennas and Propagation of College of Electronic Science and Technology, Shenzhen University. His research interests are wideband antenna, MIMO antenna, and wireless network optimization. He has authored over ten SCI and EI indexed papers, and has five invention patents. He is the Peer Reviewer of several IEEE/IET journals and conferences.

• • •